



[Direct deposition of graphene nanowalls on the ceramic powders for the fabrication of ceramic matrix composite](#)

Hai-Tao Zhou(周海涛), Da-Bo Liu(刘大博), Fei Luo(罗飞), Ye Tian(田野), Dong-Sheng Chen(陈冬生), Bing-Wei Luo(罗炳威), Zhang Zhou(周璋), Cheng-Min Shen(申承民)

Citation: Chin. Phys. B . 2019, 28(6): 068102. **doi:** 10.1088/1674-1056/28/6/068102

Journal homepage: <http://cpb.iphy.ac.cn>; <http://iopscience.iop.org/cpb>

What follows is a list of articles you may be interested in

[Superlubricity enabled dry transfer of non-encapsulated graphene](#)

Zhe Ying(应哲), Aolin Deng(邓奥林), Bosai Lyu(吕博赛), Lele Wang(王乐乐), Takashi Taniguchi, Kenji Watanabe, Zhiwen Shi(史志文)

Chin. Phys. B . 2019, 28(2): 028102. **doi:** 10.1088/1674-1056/28/2/028102

[Electronic, optical property and carrier mobility of graphene, black phosphorus, and molybdenum disulfide based on the first principles](#)

Congcong Wang(王聪聪), Xuesheng Liu(刘学胜), Zhiyong Wang(王智勇), Ming Zhao(赵明), Huan He(何欢), Jiyue Zou(邹吉跃)

Chin. Phys. B . 2018, 27(11): 118106. **doi:** 10.1088/1674-1056/27/11/118106

[Dynamically tunable terahertz passband filter based on metamaterials integrated with a graphene middle layer](#)

MaoSheng Yang(杨茂生), LanJu Liang(梁兰菊), DeQuan Wei(韦德泉), Zhang Zhang(张璋), Xin Yan(闫昕), Meng Wang(王猛), JianQuan Yao(姚建铨)

Chin. Phys. B . 2018, 27(9): 098101. **doi:** 10.1088/1674-1056/27/9/098101

[Novel graphene enhancement nanolaser based on hybrid plasmonic waveguides at optical communication wavelength](#)

Zhengjie Xu(徐政杰), Jun Zhu(朱君), Wenju Xu(徐汶菊), Deli Fu(傅得立), Cong Hu(胡聪), Frank Jiang

Chin. Phys. B . 2018, 27(8): 088104. **doi:** 10.1088/1674-1056/27/8/088104

[Modulated thermal transport for flexural and in-plane phonons in double-stub graphene nanoribbons](#)

Chang-Ning Pan(潘长宁), Meng-Qiu Long(龙孟秋), Jun He(何军)

Chin. Phys. B . 2018, 27(8): 088101. **doi:** 10.1088/1674-1056/27/8/088101

CPB

Chinese Physics B

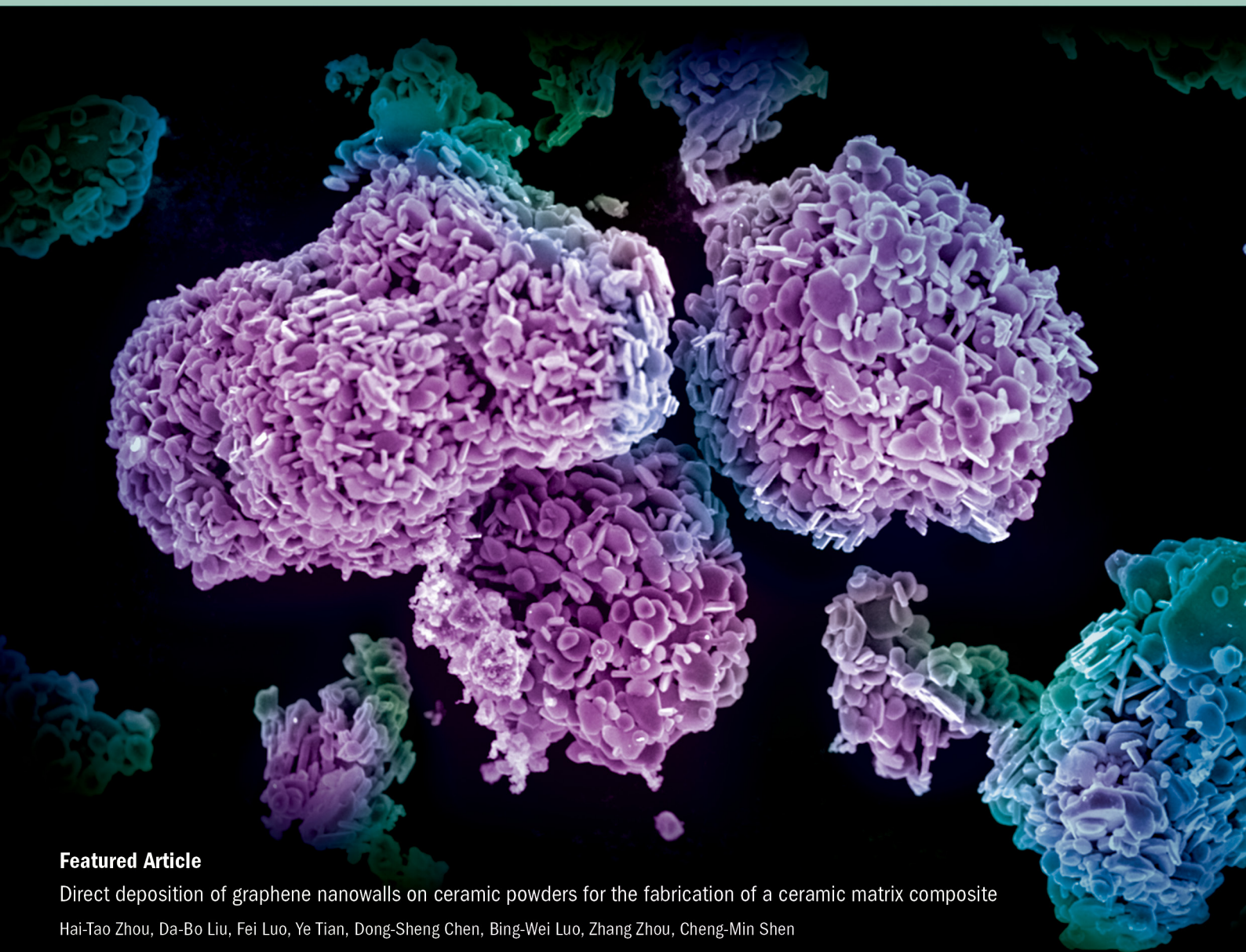
Volume 28 June 2019 Number 6

TOPICAL REVIEW

- Topological superconductors

A series Journal of the Chinese Physical Society Distributed by IOP Publishing

iopscience.org/cpb | cpb.iphy.ac.cn



Featured Article

Direct deposition of graphene nanowalls on ceramic powders for the fabrication of a ceramic matrix composite

Hai-Tao Zhou, Da-Bo Liu, Fei Luo, Ye Tian, Dong-Sheng Chen, Bing-Wei Luo, Zhang Zhou, Cheng-Min Shen

Chin. Phys. B, 2019, 28 (6): 068102

Chinese Physics B (中国物理 B)

Published monthly in hard copy by the Chinese Physical Society and online by IOP Publishing, Temple Circus, Temple Way, Bristol BS1 6HG, UK

Institutional subscription information: 2019 volume

For all countries, except the United States, Canada and Central and South America, the subscription rate per annual volume is UK£974 (electronic only) or UK£1063 (print + electronic).

Delivery is by air-speeded mail from the United Kingdom.

Orders to:

Journals Subscription Fulfilment, IOP Publishing, Temple Circus, Temple Way, Bristol BS1 6HG, UK

For the United States, Canada and Central and South America, the subscription rate per annual volume is US\$1925 (electronic only) or US\$2100 (print + electronic). Delivery is by transatlantic airfreight and onward mailing.

Orders to: IOP Publishing, P. O. Box 320, Congers, NY 10920-0320, USA

© 2019 Chinese Physical Society and IOP Publishing Ltd

All rights reserved. No part of this publication may be reproduced, stored in a retrieval system, or transmitted in any form or by any means, electronic, mechanical, photocopying, recording or otherwise, without the prior written permission of the copyright owner.

Supported by the China Association for Science and Technology and Chinese Academy of Sciences

Editorial Office: Institute of Physics, Chinese Academy of Sciences, P. O. Box 603, Beijing 100190, China

Tel: (86-10) 82649026 or 82649519, Fax: (86-10) 82649027, E-mail: cpb@aphy.iphy.ac.cn

主管单位: 中国科学院

国际统一刊号: ISSN 1674-1056

主办单位: 中国物理学会和中国科学院物理研究所

国内统一刊号: CN 11-5639/O4

主 编: 欧阳钟灿

编辑部地址: 北京 中关村 中国科学院物理研究所内

出 版: 中国物理学会

通 讯 地 址: 100190 北京 603 信箱

印刷装订: 北京科信印刷有限公司

电 话: (010) 82649026, 82649519

编 辑: Chinese Physics B 编辑部

传 真: (010) 82649027

国内发行: Chinese Physics B 出版发行部

“Chinese Physics B”网址:

国外发行: IOP Publishing Ltd

<http://cpb.iphy.ac.cn>

发行范围: 公开发刊

<http://iopscience.iop.org/journal/1674-1056>

Published by the Chinese Physical Society

Advisory Board

Prof. Academician Chen Jia-Er(陈佳洱)

School of Physics, Peking University, Beijing 100871, China

Prof. Academician Feng Duan(冯端)

Department of Physics, Nanjing University, Nanjing 210093, China

Prof. Academician T. D. Lee(李政道)

Department of Physics, Columbia University, New York, NY 10027, USA

Prof. Academician Samuel C. C. Ting(丁肇中)

LEP3, CERN, CH-1211, Geneva 23, Switzerland

Prof. Academician C. N. Yang(杨振宁)

Institute for Theoretical Physics, State University of New York, USA

Prof. Academician Yang Fu-Jia(杨福家)

Department of Nuclear Physics, Fudan University, Shanghai 200433, China

Prof. Academician Zhou Guang-Zhao
(Chou Kuang-Chao)(周光召)

China Association for Science and Technology, Beijing 100863, China

Prof. Academician Wang Nai-Yan(王乃彦)

China Institute of Atomic Energy, Beijing 102413, China

Prof. Academician Liang Jing-Kui(梁敬魁)

Institute of Physics, Chinese Academy of Sciences, Beijing 100190, China

Editor-in-Chief

Prof. Academician Ouyang Zhong-Can(欧阳钟灿)

Institute of Theoretical Physics, Chinese Academy of Sciences, Beijing 100190, China

Associate Editors

Prof. Academician Zhao Zhong-Xian(赵忠贤)
Prof. Academician Yang Guo-Zhen(杨国桢)
Prof. Academician Zhang Jie(张杰)
Prof. Academician Xing Ding-Yu(邢定钰)
Prof. Academician Shen Bao-Gen(沈保根)
Prof. Academician Gong Qi-Huang(龚旗煌)
Prof. Academician Xue Qi-Kun(薛其坤)
Prof. Sheng Ping(沈平)

Institute of Physics, Chinese Academy of Sciences, Beijing 100190, China
Institute of Physics, Chinese Academy of Sciences, Beijing 100190, China
Chinese Academy of Sciences, Beijing 100864, China
Department of Physics, Nanjing University, Nanjing 210093, China
Institute of Physics, Chinese Academy of Sciences, Beijing 100190, China
School of Physics, Peking University, Beijing 100871, China
Department of Physics, Tsinghua University, Beijing 100084, China
The Hong Kong University of Science & Technology, Kowloon, Hong Kong, China

Editorial Board

Prof. David Andelman
Prof. Academician Chen Xian-Hui(陈仙辉)

Prof. Cheng Jian-Chun(程建春)
Prof. Chia-Ling Chien

School of Physics and Astronomy Tel Aviv University, Tel Aviv 69978, Israel
Department of Physics, University of Science and Technology of China, Hefei 230026, China

Prof. Dai Xi(戴希)
Prof. Ding Jun(丁军)

School of Physics, Nanjing University, Nanjing 210093, China
Department of Physics and Astronomy, The Johns Hopkins University, Baltimore, MD 21218, USA

Prof. Masao Doi

Institute of Physics, Chinese Academy of Sciences, Beijing 100190, China
Department of Materials Science & Engineering, National University of Singapore, Singapore 117576, Singapore
Toyota Physical and Chemical Research Institute, Yokomichi, Nagakute, Aichi 480-1192, Japan

Prof. Fang Zhong(方忠)
Prof. Feng Shi-Ping(冯世平)
Prof. Academician Gao Hong-Jun(高鸿钧)
Prof. Gu Chang-Zhi(顾长志)
Prof. Gu Min(顾敏)

Institute of Physics, Chinese Academy of Sciences, Beijing 100190, China
Department of Physics, Beijing Normal University, Beijing 100875, China
Institute of Physics, Chinese Academy of Sciences, Beijing 100190, China
Institute of Physics, Chinese Academy of Sciences, Beijing 100190, China
Royal Melbourne Institute of Technology (RMIT University), GPO Box 2476, Melbourne, VIC 3001, Australia

Prof. Academician Guo Guang-Can(郭光灿)

School of Physical Sciences, University of Science and Technology of China, Hefei 230026, China

Prof. Academician He Xian-Tu(贺贤土)

Institute of Applied Physics and Computational Mathematics, Beijing 100088, China

Prof. Werner A. Hofer

Stephenson Institute for Renewable Energy, The University of Liverpool, Liverpool L69 3BX, UK

Prof. Hong Ming-Hui(洪明辉)

Department of Electrical and Computer Engineering, National University of Singapore, Singapore 117576, Singapore

Prof. Hu Gang(胡岗)

Department of Physics, Beijing Normal University, Beijing 100875, China

Prof. Jiang Hong-Wen(姜弘文)

Department of Physics and Astronomy, University of California, Los Angeles, CA 90095, USA

Prof. Jiang Ying(江颖)

School of Physics, Peking University, Beijing 100871, China

Prof. Jin Xiao-Feng(金晓峰)

Department of Physics, Fudan University, Shanghai 200433, China

Prof. Robert J. Joynt

Physics Department, University of Wisconsin-Madison, Madison, USA

Prof. Jaewan Kim

Korea Institute for Advanced Study, School of Computational Sciences, Hoegiro 85, Seoul 02455, Korea

Prof. Li Ru-Xin(李儒新)

Shanghai Institute of Optics and Fine Mechanics, Chinese Academy of Sciences, Shanghai 201800, China

Prof. Li Xiao-Guang(李晓光)

Department of Physics, University of Science and Technology of China, Hefei 230026, China

Assits. Prof. Liu Chao-Xing(刘朝星)

Department of Physics, Pennsylvania State University, PA 16802-6300, USA

Prof. Liu Xiang-Yang(刘向阳)

Department of Physics, Xiamen University, Xiamen 361005, China

Prof. Liu Ying(刘荧)

Department of Physics and Astronomy, Shanghai Jiao Tong University, Shanghai 200240, China

Prof. Long Gui-Lu(龙桂鲁)

Department of Physics, Tsinghua University, Beijing 100084, China

Prof. Lv Li(吕力)

Institute of Physics, Chinese Academy of Sciences, Beijing 100190, China

Prof. Ma Xu-Cun(马旭村)

Department of Physics, Tsinghua University, Beijing 100084, China

Prof. Antonio H. Castro Neto

Physics Department, Faculty of Science, National University of Singapore, Singapore 117546, Singapore

Prof. Nie Yu-Xin(聂玉昕)

Institute of Physics, Chinese Academy of Sciences, Beijing 100190, China

Prof. Niu Qian(牛谦)

Department of Physics, University of Texas, Austin, TX 78712, USA

Prof. Academician Ouyang Qi(欧阳颀)

School of Physics, Peking University, Beijing 100871, China

Prof. Academician Pan Jian-Wei(潘建伟)	Department of Modern Physics, University of Science and Technology of China, Hefei 230026, China
Prof. Amalia Patane	School of Physics and Astronomy, The University of Nottingham, NG7 2RD, UK
Prof. Qian Lie-Jia(钱列加)	Department of Physics and Astronomy, Shanghai Jiao Tong University, Shanghai 200240, China
Prof. J. Y. Rhee	Department of Physics, Sungkyunkwan University, Suwon, Korea
Prof. Shen Jian(沈健)	Department of Physics, Fudan University, Shanghai 200433, China
Prof. Shen Yuan-Rang(沈元壤)	Lawrence Berkeley National Laboratory, Berkeley, CA 94720, USA
Prof. Shen Zhi-Xun(沈志勋)	Stanford University, Stanford, CA 94305-4045, USA
Prof. Academician Sun Chang-Pu(孙昌璞)	Beijing Computational Science Research Center, China Academy of Engineering Physics, Beijing 100094, China
Prof. Sun Xiao-Wei(孙小卫)	Department of Electrical and Electronic Engineering, Southern University of Science and Technology, Shenzhen 518055, China
Prof. Sun Xiu-Dong(孙秀冬)	Department of Physics, Harbin Institute of Technology, Harbin 150001, China
Prof. Michiyoshi Tanaka	Research Institute for Scientific Measurements, Tohoku University, Katahira 2-1-1, Aoba-ku 980, Sendai, Japan
Prof. Tong Li-Min(童利民)	Department of Optical Engineering, Zhejiang University, Hangzhou 310027, China
Prof. Tong Peng'er(童彭尔)	Department of Physics, The Hong Kong University of Science and Technology, Kowloon, Hong Kong, China
Prof. Wang Bo-Gen(王伯根)	School of Physics, Nanjing University, Nanjing 210093, China
Prof. Wang Kai-You(王开友)	Institute of Semiconductors, Chinese Academy of Sciences, Beijing 100083, China
Prof. Wang Wei(王炜)	School of Physics, Nanjing University, Nanjing 210093, China
Prof. Wang Ya-Yu(王亚愚)	Department of Physics, Tsinghua University, Beijing 100084, China
Prof. Wang Yu-Peng(王玉鹏)	Institute of Physics, Chinese Academy of Sciences, Beijing 100190, China
Prof. Wang Zhao-Zhong(王肇中)	Laboratory for Photonics and Nanostructures (LPN) CNRS-UPR20, Route de Nozay, 91460 Marcoussis, France
Prof. Academician Wang Wei-Hua(汪卫华)	Institute of Physics, Chinese Academy of Sciences, Beijing 100190, China
Prof. Wei Su-Huai(魏苏淮)	Beijing Computational Science Research Center, China Academy of Engineering Physics, Beijing 100094, China
Prof. Wen Hai-Hu(闻海虎)	Department of Physics, Nanjing University, Nanjing 210093, China
Prof. Wu Nan-Jian(吴南健)	Institute of Semiconductors, Chinese Academy of Sciences, Beijing 100083, China
Prof. Academician Xia Jian-Bai(夏建白)	Institute of Semiconductors, Chinese Academy of Sciences, Beijing 100083, China
Prof. Academician Xiang Tao(向涛)	Institute of Physics, Chinese Academy of Sciences, Beijing 100190, China
Prof. Academician Xie Si-Shen(解思深)	Institute of Physics, Chinese Academy of Sciences, Beijing 100190, China
Prof. Academician Xie Xin-Cheng(谢心澄)	Department of Physics, Peking University, Beijing 100871, China
Prof. Academician Xu Zhi-Zhan(徐至展)	Shanghai Institute of Optics and Fine Mechanics, Chinese Academy of Sciences, Shanghai 201800, China
Assist. Prof. Xu Cen-Ke(许岑珂)	Department of Physics, University of California, Santa Barbara, CA 93106, USA
Prof. Academician Ye Chao-Hui(叶朝辉)	Wuhan Institute of Physics and Mathematics, Chinese Academy of Sciences, Wuhan 430071, China
Prof. Ye Jun(叶军)	Department of Physics, University of Colorado, Boulder, Colorado 80309-0440, USA
Prof. Yu Ming-Yang(郁明阳)	Theoretical Physics I, Ruhr University, D-44780 Bochum, Germany
Prof. Academician Zhan Wen-Long(詹文龙)	Chinese Academy of Sciences, Beijing 100864, China
Prof. Zhang Fu-Chun(张富春)	Kavli Institute for Theoretical Sciences, University of Chinese Academy of Sciences, Beijing 100190, China
Prof. Zhang Xiang(张翔)	NSF Nanoscale Science and Engineering Center (NSEC), University of California, Berkeley, CA 94720, USA
Prof. Zhang Yong(张勇)	Electrical and Computer Engineering Department, The University of North Carolina at Charlotte, Charlotte, USA
Prof. Zhang Zhen-Yu(张振宇)	International Center for Quantum Design of Functional Materials, University of Science and Technology of China, Hefei 230026, China
Prof. Zeng Hao(曾浩)	Department of Physics, University at Buffalo, SUNY, Buffalo, NY 14260, USA
Prof. Zheng Bo(郑波)	Physics Department, Zhejiang University, Hangzhou 310027, China
Prof. Zhou Xing-Jiang(周兴江)	Institute of Physics, Chinese Academy of Sciences, Beijing 100190, China
Prof. Academician Zhu Bang-Fen(朱邦芬)	Department of Physics, Tsinghua University, Beijing 100084, China

Editorial Staff

Wang Jiu-Li(王久丽) (Editorial Director) Cai Jian-Wei(蔡建伟) Zhai Zhen(翟振)

Direct deposition of graphene nanowalls on ceramic powders for the fabrication of a ceramic matrix composite*

Hai-Tao Zhou(周海涛)¹, Da-Bo Liu(刘大博)¹, Fei Luo(罗飞)¹, Ye Tian(田野)¹, Dong-Sheng Chen(陈冬生)¹, Bing-Wei Luo(罗炳威)^{1,†}, Zhang Zhou(周璋)², and Cheng-Min Shen(申承民)^{2,‡}

¹Beijing Institute of Aeronautical Materials, Aero Engine Corporation of China, Beijing 100095, China

²Beijing National Laboratory of Condensed Matter Physics, Institute of Physics, Chinese Academy of Sciences, Beijing 100190, China

(Received 28 March 2019; revised manuscript received 3 April 2019; published online 8 May 2019)

Uniform mixing of ceramic powder and graphene is of great importance for producing ceramic matrix composite. In this study, graphene nanowalls (GNWs) are directly deposited on the surface of Al_2O_3 and Si_3N_4 powders using chemical vapor deposition system to realize the uniform mixing. The morphology and the initial stage of the growth process are investigated. It is found that the graphitic base layer is initially formed parallel to the powder surface and is followed by the growth of graphene nanowalls perpendicular to the surface. Moreover, the lateral length of the graphene sheet could be well controlled by tuning the growth temperature. GNWs/ Al_2O_3 powder is consolidated by using sparking plasma sintering method and several physical properties are measured. Owing to the addition of GNWs, the electrical conductivity of the bulk alumina is significantly increased.

Keywords: graphene, ceramic matrix composite, chemical vapor deposition

PACS: 81.05.ue, 81.05.Mh, 81.15.Gh

DOI: 10.1088/1674-1056/28/6/068102

1. Introduction

Monolithic ceramics are widely used in the materials industry, including wear-resistance parts, electronics, and various coatings. However, their applications are significantly limited by the brittleness and poor electrical conductivity. To overcome these drawbacks, ceramic composites have been developed by incorporating nanofillers into the ceramic matrices.^[1–6] Recently, graphene has been widely investigated as a good filler for producing highly tough and stiff ceramic matrix composite (CMC).^[7–15] According to the papers reported in this field, the main challenges have been to produce high quality graphene and realize good dispersion of graphene in ceramic matrix. In these studies, ball-milling^[7–12] and colloidal processing^[13–15] were two mainly used mixing methods. Ball-milling technique imposed heavy shear forces on graphene to break its agglomeration and promote its dispersion. Colloidal processing produced well dispersed mixture usually by adding graphene oxide (GO) dropwise into ceramic suspension under magnetic stirring. However, the severe collision in ball-milling and the oxidation treatment in preparing GO by hummer's method would all significantly damage the graphene flakes and give rise to massive structural defects,^[16,17] which degraded the physical properties in contrast with pure graphene. To produce high quality CMC, it is necessary to develop a new method to realize better control of

the quality of graphene, as well as uniform mixing.

Recent years have witnessed great progress in the growth of graphene nanowalls (GNWs) on arbitrary substrates by employing plasma-enhanced chemical vapor deposition (PECVD) technique.^[18–23] This method enables the low-temperature and uniform synthesis of graphene nanosheets owing to the presence of reactive species generated in the plasma region, and the GNWs have been widely used in the aspects of solar cells, supercapacitor, and field emission.^[19,20,22] In this study, we aim to utilize PECVD to directly deposit graphene on the surface of ceramic powder, and the morphology and the initial stage of growth process of GNWs have been investigated.

2. Experimental procedure

2.1. Growth of GNWs on the ceramic powder

The α -alumina powder (Xilong Scientific Ltd.) with a purity of 99.85% and an average particle size of 50 μm was studied. GNWs were deposited in a remote radio-frequency (RF) PECVD system. Thin powder layer was flatly laid in the bottom of the crucible and then transferred into the quartz tube furnace. Prior to deposition, the furnace was pumped down to a pressure of 5×10^{-1} Pa, then the temperature was raised to 600 °C or 700 °C at a rate of 20 °C/min under the protection of Ar flow of 150 standard cubic centimeters per minute

*Project supported by the National Natural Science Foundation of China (Grant Nos. 51602300 and 51602299) and the National Key Research and Development Program of China (Grant No. 2018FYA0305800).

[†]Corresponding author. E-mail: luobingwei@126.com

[‡]Corresponding author. E-mail: cmsen@iphy.ac.cn

© 2019 Chinese Physical Society and IOP Publishing Ltd

<http://iopscience.iop.org/cpb> <http://cpb.iphy.ac.cn>

(sccm). Thereafter, CH_4 flow (20 sccm) was introduced into the furnace and 290 W RF was generated simultaneously. After the deposition, the RF and CH_4 flow were turned off and the ceramic powder was naturally cooled down to room temperature.

2.2. Spark plasma sintering (SPS)

Bulk ceramic composite was fabricated using an SPS-1050 T apparatus. The powder was loaded in a cylindrical graphite die with an inner diameter of 40 mm. Two graphite plungers were used to seal the die on both ends. The sintering process was carried out under a vacuum of 5 Pa and a uniaxial pressure of 4 MPa was applied. Samples were heated to 1450 °C at a rate of 10 °C/min. The dwelling time was 5 minutes.

2.3. Characterizations

The microstructure of the powder was characterized by scanning electron microscope (SEM, Hitachi S-4800) and high resolution transmission electron microscope (HRTEM, FEI Tecai G2F20). Raman spectrum was recorded on the Horiba Jobin Yvon LabRAM HR-800 with a laser wavelength of 532 nm and an incident power of 1 mW. The x-ray photoelectron spectroscopy (XPS) analysis was carried out on Thermo

escalab 250XI, using monochromatized Al $K\alpha$ radiation at 150 W. The high resolution XPS spectra were recorded in the constant analyzer energy (CAE) mode with a pass energy of 20 eV and a step size of 0.1 eV. The density values were measured using the Archimedes method. Vecker hardness tests were carried out on the Future-Tech with a 100-g force. Keysight 2902A was used to measure the conductivity at 25 °C on a small piece of sample with a size of 8 mm×8 mm×0.5 mm.

3. Results and discussion

Figure 1(a) shows a schematic illustration of the remote PECVD system, in which the RF helical-coil is mounted at the upstream side and could dissociate the methane gas into various active radicals. Owing to these radicals, the growth of GNWs does not depend on the catalytic decomposition of the precursor by the metallic substrate and could be realized on almost arbitrary substrates from metal to insulator, such as copper, silicon, and glass.^[22,24,25] Figure 1(b) shows a comparison photograph, from which we could clearly find that the alumina (Al_2O_3) powder completely turns black after the GNWs deposition of 90 min. Raman spectrum in Fig. 1(c) verifies the

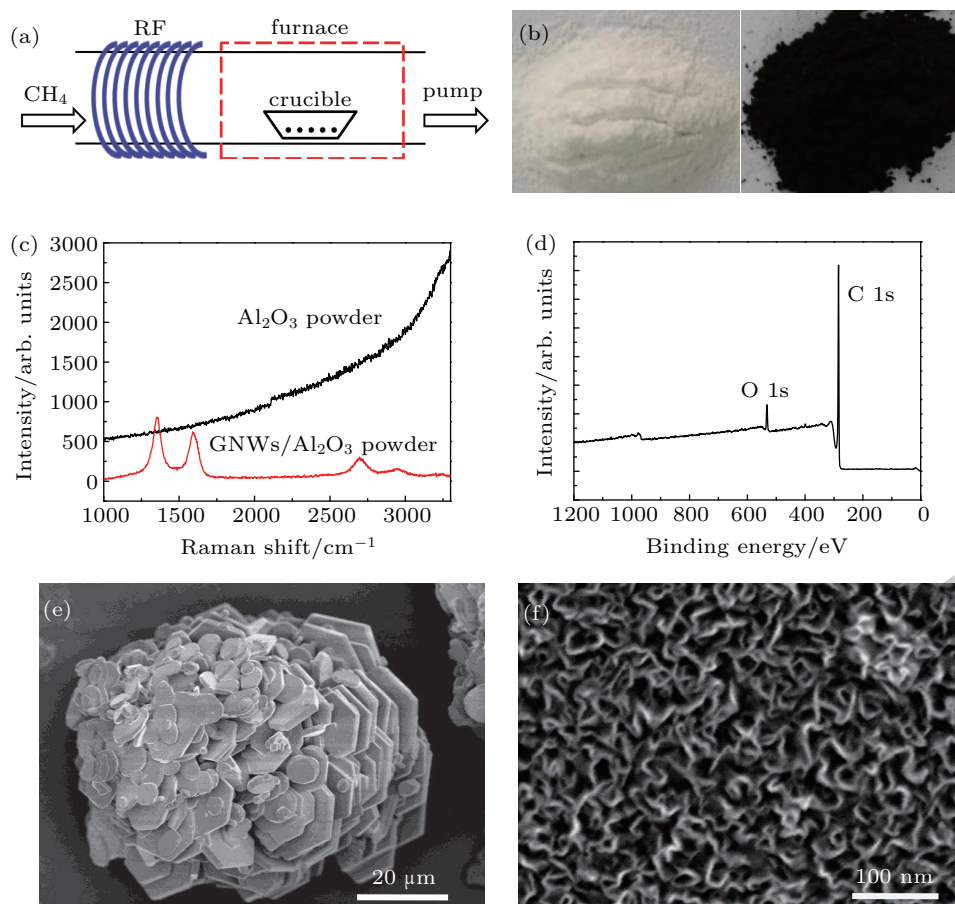


Fig. 1. (a) Schematic illustration of PECVD system. (b) Photographs of Al_2O_3 powder before (left) and after (right) GNWs deposition. (c) Raman spectrum. (d) XPS of GNWs/ Al_2O_3 powder. (e) Low-magnification SEM image showing overall view of Al_2O_3 particles. (f) High-magnification image showing GNWs on the particle. Graphene deposition parameter: 700 °C, 290 W, 90 min.

formation of GNWs and presents three intrinsic peaks located at 1353 cm^{-1} , 1590 cm^{-1} , and 2697 cm^{-1} , corresponding to D band, G band, and 2D band of grapheme, respectively.^[26,27] XPS analysis is used to study the chemical composition of the GNWs. Figure 1(d) is a representative spectrum, showing a strong C 1s peak at 284.8 eV and a small O 1s peak at 532.5 eV. No other elements are detected in the GNWs except for some oxygen adsorbates. The existence of these oxygen adsorbates is due to the physical and/or chemical adsorption of oxygen when the sample is exposed to ambient conditions.

The large-scale SEM image in Fig. 1(e) is an overall view of a single alumina particle. The particle has a size of $\sim 50\text{ }\mu\text{m}$ and consists of numerous alumina pieces. The morphology and structure of the GNWs-capping on the alumina particle are analyzed by the SEM and HRTEM techniques. From the higher-magnification SEM image (Fig. 1(f)), GNWs could be clearly identified, showing a curled-sheet feature and an average length of $\sim 70\text{ nm}$. According to the previous report, GNWs are composed of two kinds of structures, named stem- and branch-structures.^[23] The graphene sheets visible in Fig. 1(f) are referred to as stem. As shown in Fig. 2(a), we could see the branches at much higher magnification, in which several stem- and branch- structures are labeled by the solid and dashed arrows, respectively. The branches are much smaller and dimmer compared with the stems. To further understand the structure of GNWs, TEM is harnessed to study the morphology. Figure 2(b) shows a typical TEM image of a single sheet of GNWs. Dense branches with the size of several nanometers could be clearly identified, and three of them are labeled by arrows to guide the eye. HRTEM images could be used to identify the graphene layers. The image (Fig. 2(c)) obtained at the edge of stem-structure indicates that this stem is terminated with two-layer graphene. The interlayer spacing between two neighboring monolayer is about 0.37 nm . This value is slightly larger than that of graphite, which is most likely due to the reduced interactions between graphene layers.^[19] Figure 2(d) shows an HRTEM image recorded in the zone of branches, from which we could find that the branches are composed of various graphene layers with an average interlayer spacing of 0.374 nm . These results imply that the GNWs films correspond to few-layer graphene.

Many efforts have been made to investigate the growth mechanism of GNWs on metallic substrates, such as Cu, Ni, and Pt.^[22,23,28] Most of these studies indicated that the growth of GNWs was composed of two stages: initially, the carbon radicals nucleated and massive graphene layers in parallel with substrate took form, following a two-dimensional (2D) growth mode; as the number of layers increased and the strain energy accumulated, 2D layers became energetically unfavorable

and a transition to three-dimensional (3D) growth took place. However, few work reported the growth mechanism on the surface of ceramics. To elucidate this issue, the growth process of GNWs is monitored by gradually varying the growth time under otherwise the same condition. Before graphene deposition, the surface of alumina particle has a clean and smooth topography, as shown in the SEM image of Fig. 3(a). After 10 min deposition (Fig. 3(b)), graphene sheets with wrinkle structures could be clearly identified. At this stage, these sheets are still lying down on the substrate. When the deposition time is elongated to 20 min (Fig. 3(c)), the transition to 3D growth occurs and some graphene sheets stand up at the substrate, as labeled by solid arrows. The above observations prove that the growth of GNWs on ceramic surface also complies well with the two-stage mode. According to this mode, we could control the lateral width of the graphene sheets by changing the growth temperature.^[22] As shown in Figs. 3(d) and 3(e), at a growth temperature of $700\text{ }^{\circ}\text{C}$, all the sheets of GNWs present similar width of 70 nm ; in contrast, the width increases to 150 nm at $600\text{ }^{\circ}\text{C}$. In ball-milling and colloidal methods, the size of graphene flakes is uncontrollable. Thus, no work so far has reported the effect of the size distribution of graphene sheets on the properties of CMC. In our experiment, the size of graphene sheets is uniform at a given growth temperature and is adjustable by changing the temperature, which makes the study of size effect feasible.

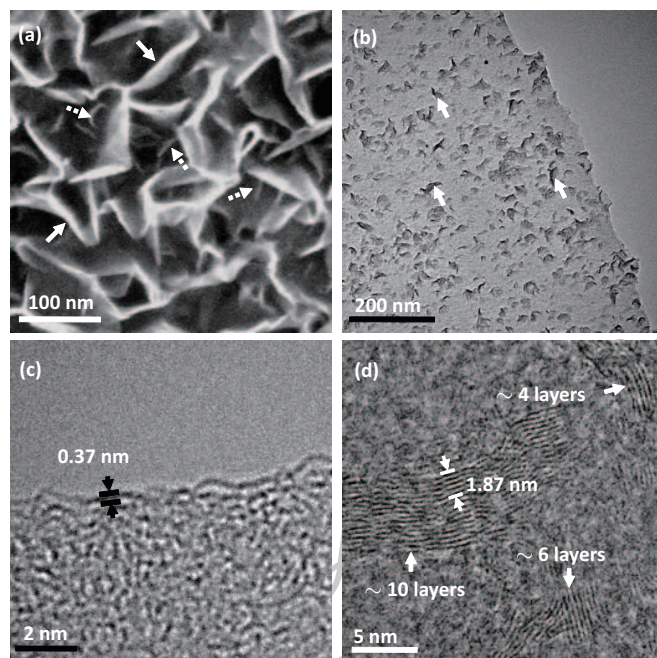


Fig. 2. (a) High-magnification SEM image showing abundant of stem- (solid arrows) and branch- (dashed arrows) structures. (b) TEM image of branches (labeled by arrows) on the stem. (c) HRTEM image at the edge of the stem, indicating the stem is terminated with two-layer graphene with an interlayer spacing of 0.37 nm . (d) HRTEM image at the branches, showing the branches are composed of various graphene layers with an average interlayer spacing of $1.87/5 = 0.374\text{ nm}$.

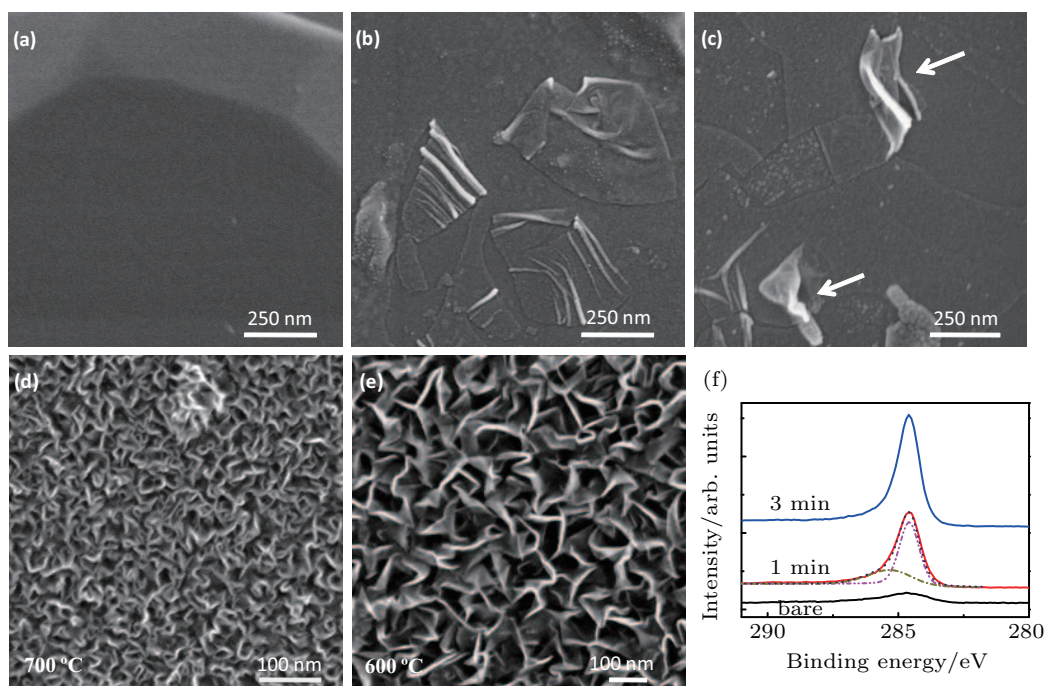


Fig. 3. (a) High-magnification SEM image of bare Al₂O₃ powder. (b) Image after 10-min deposition showing 2D graphene layers. (c) Image after 20-min deposition showing the transition to 3D graphene layers. (d) and (e) Graphene sheets showing variable lateral lengths at different growth temperatures. (f) High-resolution XPS spectra recorded after different deposition times. Graphene deposition parameters are: (b)–(d) 700 °C, 290 W; (e) 600 °C, 290 W.

XPS measurements are also carried out to detect the growth process of GNWs. Before deposition, the bare Al₂O₃ powder is treated at ambient atmosphere at 800 °C for three hours. Our results indicate that the content of residual amorphous carbon significantly decreases from 12.3 at.% to 7.1 at.% after this treatment. The high-resolution C 1s spectra recorded at different deposition times are presented in Fig. 3(f). The amorphous carbon on bare Al₂O₃ powder shows a broad C 1s peak and a maximum at 284.68 eV. The peak recorded after 1-min deposition is obviously different, which is located at 284.79 eV and shows a characteristic shape of C 1s spectrum of graphitic carbon. This peak could be fitted with two peaks at 284.8 eV and 285.5 eV, corresponding to graphitic carbon and C–O bond, respectively. The existence of C–O bond might be due to the fact that the carbon radicals partially reduce the Al₂O₃ surface and the Al–O–C bonds form.^[29] There is almost no change in the shape of C 1s when the deposition time is elongated to 3 min. The carbon concentrations measured on the powder surface are 34 at.% and 48 at.% after 1-min and 3-min depositions, respectively.

To elucidate the universality and advantage of our method, we further deposit GNWs on the surface of silicon nitride (Si₃N₄). As shown in the SEM image of Fig. 4(a), the Si₃N₄ powder shows a particle size of below 3 μm. At higher magnification, graphene sheets could be identified with an average length of 70 nm and 150 nm at the growth temperature of 700 °C (Fig. 4(b)) and 600 °C (Fig. 4(c)), respectively. The

Raman spectrum in Fig. 4(d) presents three peaks located at 1350 cm⁻¹ (D), 1586 cm⁻¹ (G), and 2702 cm⁻¹ (2D), further verifying the formation of GNWs. The results are similar to these on alumina powder, indicating that the growth of GNWs is independent on the type of ceramic powder and could be further extended to other powders such as SiC, SiO₂, and mullite.

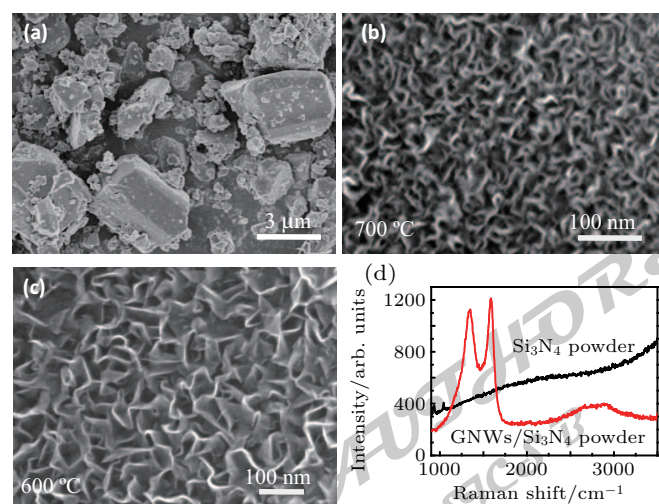


Fig. 4. (a) Low-magnification SEM image showing overall view of Si₃N₄ particles. (b) and (c) High-magnification image of GNWs on the particle, showing variable lateral lengths at different growth temperatures. (d) Raman spectrum. Graphene deposition parameters are: (b) 700 °C, 290 W, 90 min; (c) 600 °C, 290 W, 90 min.

The GNWs-Al₂O₃ powder is sintered by SPS method to fabricate alumina composite. The volume percent of graphene in this sample is about 0.25%. Pure Al₂O₃ powder is also

sintered to bulk monolithic alumina using the same condition for comparison. The composite has a black color, exhibiting a sharp contrast with the white monolithic alumina. Graphene owns exceptional high electrical conductivity and is considered to be an ideal additive to improve this property of ceramic.^[7,16,30] We carry out measurements on several physical properties such as bulk density, Vickers hardness, and electrical conductivity. The monolithic alumina and the composite exhibit similar bulk density with the value of 3.899 g/cm³ and 3.918 g/cm³, respectively. These numbers are very close to the ideal value of alumina (3.97 g/cm³), indicating that the sintering parameters used in our experiment are suitable. There are little differences in hardness between the two samples, with the value of 1667 HV and 1652 HV, respectively. However, the addition of graphene could significantly raise the electrical conductivity of alumina. Our experiment results show that the monolithic Al₂O₃ is an insulator. The graphene sheets in the composite provide numerous conductive paths and sharply increase the electrical conductivity to a value of 0.724 S/m.

4. Conclusion and perspectives

GNWs film has been successfully deposited on the surface of Al₂O₃ and Si₃N₄ powders. The layers, counted from HRTEM images, imply that the GNWs correspond to few-layer graphene. SEM results indicate that the growth process includes a transition from 2D to 3D mode at the initial stage. The lateral length of graphene sheets could be well controlled by changing the deposition temperature, which is about 70 nm and 150 nm at 700 °C and 600 °C, respectively. Moreover, the electrical conductivity of the composite significantly increases compared with the monolithic alumina. Our experiment provides an alternative way to realize the uniform mixing of graphene and ceramic powders, which has potential applications in fabricating ceramic matrix composites.

References

- [1] Inam F, Yan H X, Jayaseelan D D, Peijs T and Reece M J 2010 *J. Eur. Ceram. Soc.* **30** 153
- [2] Cho J, Boccaccini A R and Shaffer M S P 2009 *J. Mater. Sci.* **44** 1934
- [3] Cho J, Inam F, Reece M J, Chlup Z, Dlouhy I, Shaffer M S P and Boccaccini A R 2011 *J. Mater. Sci.* **46** 4770
- [4] Wu Y and Kim G Y 2011 *J. Mater. Process. Technol.* **211** 1341
- [5] Esawi A and Morsi K 2007 *Compos. Part. A* **38** 646
- [6] Esawi A M K, Morsi K, Sayed A, Taher M and Lanka S 2011 *Compos. Part. A* **42** 234
- [7] Fan Y C, Wang L J, Li J L, Li J Q, Sun S K, Chen F, Chen L D and Jiang W 2010 *Carbon* **48** 1743
- [8] He T, Li J L, Wang L J, Zhu J J and Jiang W 2009 *Mater. Trans.* **50** 749
- [9] Tapasztó O, Tapasztó L, Marko M, Kern F, Gadow R and Balazsi C 2011 *Chem. Phys. Lett.* **511** 340
- [10] Liu J, Yan H X and Jiang K 2013 *Ceram. Int.* **39** 6215
- [11] Cygan T, Wozniak J, Kostecki M, Petrus M, Jastrzębska A, Ziemkowska W and Olszyna A 2017 *Ceram. Int.* **43** 6180
- [12] Sedlák R, Kovalčíková A, Múdra E, Rutkowski P, Dubiel A, Girman V, Bystrický R and Duszka J 2017 *J. Eur. Ceram. Soc.* **37** 3773
- [13] Walker L S, Marotto V R, Rafiee M A, Koratkar N and Corral E L 2011 *ACS Nano* **5** 3182
- [14] Wang K, Wang Y F, Fan Z J, Yan J and Wei T 2011 *Mater. Res. Bull.* **46** 315
- [15] Gutierrez-Gonzalez C F, Smirnov A, Centeno A, Fernández A, Alonso B, Rocha V G, Torrecillas R, Zurutuza A and Bartolome J F 2015 *Ceram. Int.* **41** 7434
- [16] Porwal H, Grasso S and Reece M J 2013 *Adv. Appl. Ceram.* **112** 443
- [17] Markandana K, Chin J K and Tan M 2017 *J. Mater. Res.* **32** 84
- [18] Zhang Y, Du J L, Tang S, Liu P, Deng S Z, Chen J and Xu N S 2012 *Nanotechnol.* **23** 015202
- [19] Jiang L L, Yang T Z, Liu F, Dong J, Yao Z H, Shen C M, Deng S Z, Xu N S, Liu Y Q and Gao H J 2013 *Adv. Mater.* **25** 250
- [20] Sun J Y, Chen Y B, Cai X, Ma B J, Chen Z L, Priyadarshi M K, Chen K, Gao T, Song X J, Ji Q Q, Guo X F, Zou D C, Zhang Y F and Liu Z F 2015 *Nano Res.* **8** 3496
- [21] Chen X D, Chen Z L, Sun J Y, Zhang Y F and Liu Z F 2016 *Acta Phys. -Chim. Sin.* **32** 14
- [22] Zhou H T, Yu N, Zou F, Yao Z H, Gao G and Shen C M 2016 *Chin. Phys. B* **25** 096106
- [23] Zhou H T, Liu D B, Luo F, Luo B W, Tian Y, Chen D S and Shen C M 2018 *Micro & Nano Lett.* **13** 842
- [24] Zou F, Zhou H T, Yu N, Yao Z H, Liu F and Shen C M 2016 *Chem. Phys. Lett.* **664** 29
- [25] Dong J, Yao Z H, Yang T Z, Jiang L L and Shen C M 2013 *Sci. Rep.* **3** 1733
- [26] Gupta A, Chen G, Joshi P, Tadigadapa S and Eklund P C 2006 *Nano Lett.* **6** 2667
- [27] Graf D, Molitor F, Ensslin K, Stampfer C, Jungen A, Hierold C and Wirtz L 2007 *Nano Lett.* **7** 238
- [28] Vitchev R, Alexander Malesev A, Petrov R, Kemps R, Mertens M, Annick Vanhulsel A and Haesendonck C 2010 *Nanotechnol.* **21** 095602
- [29] Zhou M, Bi H, Lin T Q, Lv X J, Wan D Y, Huang F Q and Lin J H 2014 *Carbon* **75** 314
- [30] Li Q S, Zhang Y J, Gong H Y, Sun H B, Li T, Guo X and Ai S H 2015 *Ceram. Int.* **41** 13547

Chinese Physics B

Volume 28

Number 6

June 2019

TOPICAL REVIEW — Topological superconductors

067403 Topological superconductivity in a $\text{Bi}_2\text{Te}_3/\text{NbSe}_2$ heterostructure: A review

Hao Zheng and Jin-Feng Jia

RAPID COMMUNICATION

065101 The universal characteristic water content of aqueous solutions

Xiao Huang, Ze-Xian Cao and Qiang Wang

067303 Neutral excitation and bulk gap of fractional quantum Hall liquids in disk geometry

Wu-Qing Yang, Qi Li, Lin-Peng Yang and Zi-Xiang Hu

068102 Direct deposition of graphene nanowalls on ceramic powders for the fabrication of a ceramic matrix composite

Hai-Tao Zhou, Da-Bo Liu, Fei Luo, Ye Tian, Dong-Sheng Chen, Bing-Wei Luo, Zhang Zhou and Cheng-Min Shen

068203 Hard carbons derived from pine nut shells as anode materials for Na-ion batteries

Hao Guo, Kai Sun, Yaxiang Lu, Hongliang Wang, Xiaobai Ma, Zhengyao Li, Yong-Sheng Hu and Dongfeng Chen

GENERAL

060201 Simulation of the influence of imperfections on dynamical decoupling of a superconducting qubit

Ying-Shan Zhang, Jian-She Liu, Chang-Hao Zhao, Yong-Cheng He, Da Xu and Wei Chen

060301 Atom interferometers with weak-measurement path detectors and their quantum mechanical analysis

Zhi-Yuan Li

060302 Spin squeezing in Dicke-class of states with non-orthogonal spinors

K S Akhilesh, K S Mallesh, Sudha and Praveen G Hegde

060303 Steady-state entanglement and heat current of two coupled qubits in two baths without rotating wave approximation

Mei-Jiao Wang and Yun-Jie Xia

060304 Entropy squeezing for three-level atom interacting with a single-mode field

Fei-Fan Liu, Mao-Fa Fang and Xiong Xu

060305 Simulation and measurement of millimeter-wave radiation from Josephson junction array

Xin Zhang, Sheng-Hui Zhao, Li-Tian Wang, Jian Xing, Sheng-Fang Zhang, Xue-Lian Liang, Ze He, Pei Wang, Xin-Jie Zhao, Ming He and Lu Ji

(Continued on the Bookbinding Inside Back Cover)

- 060501 Group consensus of multi-agent systems subjected to cyber-attacks**
Hai-Yun Gao, Ai-Hua Hu, Wan-Qiang Shen and Zheng-Xian Jiang
- 060502 Domain walls and their interactions in a two-component Bose–Einstein condensate**
Ling-Zheng Meng, Yan-Hong Qin, Li-Chen Zhao and Zhan-Ying Yang
- 060701 Thermal characterization of GaN heteroepitaxies using ultraviolet transient thermoreflectance**
Kang Liu, Jiwen Zhao, Huarui Sun, Huaixin Guo, Bing Dai and Jiaqi Zhu
- 060702 Investigation of copper sulfate pentahydrate dehydration by terahertz time-domain spectroscopy**
Yuan-Yuan Ma, Hao-Chong Huang, Si-Bo Hao, Wei-Chong Tang, Zhi-Yuan Zheng and Zi-Li Zhang
- 060703 Digitally calibrated broadband dual-comb gases absorption spectral measurements**
Xinyi Chen, Weipeng Zhang, Haoyun Wei and Yan Li
- 060704 Negativity of Wigner function and phase sensitivity of an SU(1,1) interferometer**
Chun-Li Liu, Li-Li Guo, Zhi-Ming Zhang and Ya-Fei Yu
- 060705 Structure, conductivity, and ion emission properties of RbAg₄I₅ solid electrolyte film prepared by pulsed laser deposition**
Jun-Lian Chen, Wen-Bin Zuo, Xian-Wen Ke, Alexander B Tolstoguzov, Can-Xin Tian, Neena Devi, Ranjana Jha, Gennady N Panin and De-Jun Fu
- 060706 New measurement of thick target yield for narrow resonance at $E_x = 9.17$ MeV in the $^{13}\text{C}(p,\gamma)^{14}\text{N}$ reaction**
Yong-Le Dang, Fu-Long Liu, Guang-Yong Fu, Di Wu, Chuang-Ye He, Bing Guo and Nai-Yan Wang
- 060707 Photo-transmutation based on resonance γ -ray source**
Guang-Yong Fu, Yong-Le Dang, Fu-Long Liu, Di Wu, Chuang-Ye He and Nai-Yan Wang

ATOMIC AND MOLECULAR PHYSICS

- 063201 Photoelectron imaging of resonance-enhanced multiphoton ionization and above-threshold ionization of ammonia molecules in a strong 800-nm laser pulse**
Le-Le Song, Ya-Nan Sun, Yan-Hui Wang, Xiao-Chun Wang, Lan-Hai He, Si-Zuo Luo, Wen-Hui Hu, Qiu-Nan Tong, Da-Jun Ding and Fu-Chun Liu
- 063202 Quantal studies of sodium $3p \leftarrow 3s$ photoabsorption spectra perturbed by ground lithium atoms**
N Lamoudi, F Talbi, M T Bouazza, M Bouledroua and K Alioua
- 063203 Charge-state populations for the neon-XFEL system**
Ping Deng and Gang Jiang
- 063301 Hydrogen sulphide detection using near-infrared diode laser and compact dense-pattern multipass cell**
Xing Tian, Yuan Cao, Jia-Jin Chen, Kun Liu, Gui-Shi Wang and Xiao-Ming Gao
- 063401 Non-adiabatic quantum dynamical studies of $\text{Na}(3p) + \text{HD}(\nu = 1, j = 0) \rightarrow \text{NaH}/\text{NaD} + \text{D}/\text{H}$ reaction**
Yue-Pei Wen, Bayaer Buren and Mao-Du Chen

**ELECTROMAGNETISM, OPTICS, ACOUSTICS, HEAT TRANSFER, CLASSICAL MECHANICS,
AND FLUID DYNAMICS**

- 064101 Axial magnetic field effect in numerical analysis of high power Cherenkov free electron laser**
F Bazouband and B Maraghechi
- 064201 Characterization of focusing performance of spiral zone plates with fractal structure**
Hua-Ping Zang, Cheng-Long Zheng, Zi-Wen Ji, Quan-Ping Fan, Lai Wei, Yong-Jie Li, Kai-Jun Mu, Shu Chen, Chuan-Ke Wang, Xiao-Li Zhu, Chang-Qing Xie, Lei-Feng Cao and Er-Jun Liang
- 064202 Fast Fourier single-pixel imaging based on Sierra-Lite dithering algorithm**
Zhen-Yu Liang, Zheng-Dong Cheng, Yan-Yan Liu, Kuai-Kuai Yu and Yang-Di Hu
- 064203 Fe:ZnSe laser pumped by a 2.93- μm Cr, Er:YAG laser**
Ying-Yi Li, Tong-Yu Dai, Xiao-Ming Duan, Chun-Fa Guo, Li-Wei Xu and You-Lun Ju
- 064204 Supercontinuum generation of highly nonlinear fibers pumped by 1.57- μm laser soliton**
Song-Tao Fan, Yan-Yan Zhang, Lu-Lu Yan, Wen-Ge Guo, Shou-Gang Zhang and Hai-Feng Jiang
- 064205 Monolithic all-fiber mid-infrared supercontinuum source based on a step-index two-mode As_2S_3 fiber**
Jinmei Yao, Bin Zhang and Jing Hou
- 064206 Analysis of third and one-third harmonic generation in lossy waveguides**
Jianyu Zhang, Yunxu Sun and Qinghai Song
- 064207 Energetic few-cycle pulse compression in gas-filled hollow core fiber with concentric phase mask**
Yu Zhao, Zhi-Yuan Huang, Rui-Rui Zhao, Ding Wang and Yu-Xin Leng
- 064208 High-performance waveguide-integrated Ge/Si avalanche photodetector with small contact angle between selectively epitaxial growth Ge and Si layers**
Xiao-Qian Du, Chong Li, Ben Li, Nan Wang, Yue Zhao, Fan Yang, Kai Yu, Lin Zhou, Xiu-Li Li, Bu-Wen Cheng and Chun-Lai Xue
- 064209 Macadam's theory in RGB laser display**
Guan Wang, Yuhua Yang, Tianhao Dong, Chun Gu, Lixin Xu, Zhongcan Ouyang and Zuyan Xu
- 064210 Internal and near-surface fields for a chiral sphere under arbitrary laser beam illumination**
Bi-Da Su, Ming-Jun Wang, Yue Peng, Su-Hui Yang and Hua-Yong Zhang
- 064401 Infrared cooling properties of cordierite**
Si-Heng Chen, Xiao-Xiong Wang, Guang-Di Nie, Qi Liu, Jin-Xia Sui, Chao Song, Jian-Wei Zhu, Jie Fu, Jun-Cheng Zhang, Xu Yan and Yun-Ze Long
- 064402 Uniformity principle of temperature difference field in heat transfer optimization**
Xue-Tao Cheng and Xin-Gang Liang
- 064403 Three-dimensional thermal illusion devices with arbitrary shape**
Xingwei Zhang, Xiao He and Linzhi Wu
- 064701 Effects of thiocyanate anions on switching and structure of poly(N-isopropylacrylamide) brushes**
Xin-Jun Zhao and Zhi-Fu Gao

064702 Flow characteristics of supersonic gas passing through a circular micro-channel under different inflow conditions

Guang-Ming Guo, Qin Luo, Lin Zhu and Yi-Xiang Bian

064703 Relationship between characteristic lengths and effective Saffman length in colloidal monolayers near a water–oil interface

Na Li, Wei Zhang and Wei Chen

064704 Studies of flow field characteristics during the impact of a gaseous jet on liquid–water column

Jian Wang, Wen-Jun Ruan, Hao Wang and Li-Li Zhang

CONDENSED MATTER: STRUCTURAL, MECHANICAL, AND THERMAL PROPERTIES

066101 Quantum density functional theory studies of structural, elastic, and opto-electronic properties of $Z\text{MoO}_3$ ($Z = \text{Ba}$ and Sr) under pressure

Saad Tariq, A A Mubarak, Saher Saad, M Imran Jamil and S M Sohail Gilani

066201 Nanosheet-structured B_4C with high hardness up to 42 GPa

Chang-Chun Wang and Le-Le Song

066301 Theoretical analysis of cross-plane lattice thermal conduction in graphite

Yun-Feng Gu

066401 Calculation of the infrared frequency and the damping constant (full width at half maximum) for metal organic frameworks

M Kurt, H Yurtseven, A Kurt and S Aksoy

066402 Pressure-induced isostructural phase transition in $\alpha\text{-Ni}(\text{OH})_2$ nanowires

Xin Ma, Zhi-Hui Li, Xiao-Ling Jing, Hong-Kai Gu, Hui Tian, Qing Dong, Peng Wang, Ran Liu, Bo Liu, Quan-Jun Li, Zhen Yao and Bing-Bing Liu

066801 Real-space observation on standing configurations of phenylacetylene on Cu (111) by scanning probe microscopy

Jing Qi, Yi-Xuan Gao, Li Huang, Xiao Lin, Jia-Jia Dong, Shi-Xuan Du and Hong-Jun Gao

066802 Formation and preferred growth behavior of grooved seed silicon substrate for kerfless technology

Jing-Yuan Yan, Yong-Wei Wang, Yong-Ming Guo, Wei Zhang, Cong Wang, Bao-Li An and Dong-Fang Liu

066803 Nonlocal effect on resonant radiation force exerted on semiconductor coupled quantum well nanostructures

Jin-Ke Zhang, Ting-Ting Zhang, Yu-Liang Zhang, Guang-Hui Wang and Dong-Mei Deng

066804 Temperature-dependent subband mobility characteristics in n-doped silicon junctionless nanowire transistor

Ya-Mei Dou, Wei-Hua Han, Yang-Yan Guo, Xiao-Song Zhao, Xiao-Di Zhang, Xin-Yu Wu and Fu-Hua Yang

CONDENSED MATTER: ELECTRONIC STRUCTURE, ELECTRICAL, MAGNETIC, AND OPTICAL PROPERTIES

067201 Magnetotransport properties of graphene layers decorated with colloid quantum dots

Ri-Jia Zhu, Yu-Qing Huang, Jia-Yu Li, Ning Kang and Hong-Qi Xu

067301 Time-dependent first-principles study of optical response of BaTiO₃ quantum dots coupled with silver nanowires

Bo-Xun Han and Hong Zhang

067302 Analysis of displacement damage effects on bipolar transistors irradiated by spallation neutrons

Yan Liu, Wei Chen, Chaohui He, Chunlei Su, Chenhui Wang, Xiaoming Jin, Junlin Li and Yuanyuan Xue

067304 Method of evaluating interface traps in Al₂O₃/AlGaIn/GaN high electron mobility transistors

Si-Qin-Gao-Wa Bao, Xiao-Hua Ma, Wei-Wei Chen, Ling Yang, Bin Hou, Qing Zhu, Jie-Jie Zhu and Yue Hao

067305 Aging mechanism of GaN-based yellow LEDs with V-pits

Tian-Ran Zhang, Fang Fang, Xiao-Lan Wang, Jian-Li Zhang, Xiao-Ming Wu, Shuan Pan, Jun-Lin Liu and Feng-Yi Jiang

067401 Crystal structures and sign reversal Hall resistivities in iron-based superconductors Li_x(C₃H₁₀N₂)_{0.32}FeSe (0.15 < x < 0.4)

Rui-Jin Sun, Shi-Feng Jin, Jun Deng, Mu-Nan Hao, Lin-Lin Zhao, Xiao Fan, Xiao-Ning Sun, Jian-Gang Guo and Lin Gu

067402 Enhancing superconductivity of ultrathin YBa₂Cu₃O_{7-δ} films by capping non-superconducting oxides

Hai Bo, Tianshuang Ren, Zheng Chen, Meng Zhang and Yanwu Xie

067501 Critical behavior and magnetocaloric effect in magnetic Weyl semimetal candidate Co_{2-x}ZrSn

Tianlin Yu, Xiaoyun Yu, En Yang, Chang Sun, Xiao Zhang and Ming Lei

067701 Fabrication and characterization of one-port surface acoustic wave resonators on semi-insulating GaN substrates

Xue Ji, Wen-Xiu Dong, Yu-Min Zhang, Jian-Feng Wang and Ke Xu

067801 Gradient refractive structured NiCr thin film absorber for pyroelectric infrared detectors

Yunlu Lian, He Yu, Zhiqing Liang and Xiang Dong

INTERDISCIPLINARY PHYSICS AND RELATED AREAS OF SCIENCE AND TECHNOLOGY

068101 Structural stability and vibrational characteristics of CaB₆ under high pressure

Mingkun Liu, Can Tian, Xiaoli Huang, Fangfei Li, Yanping Huang, Bingbing Liu and Tian Cui

068103 Fluorescence spectra of colloidal self-assembled CdSe nano-wire on substrate of porous Al₂O₃/Au nanoparticles

Xin Zhang, Li-Ping Shao, Man Peng, Zhong-Chen Bai, Zheng-Ping Zhang and Shui-Jie Qin

068104 Spin glassy behavior and large exchange bias effect in cubic perovskite Ba_{0.8}Sr_{0.2}FeO_{3-δ}

Yu-Xuan Liu, Zhe-Hong Liu, Xu-Bin Ye, Xu-Dong Shen, Xiao Wang, Bo-Wen Zhou, Guang-Hui Zhou and You-Wen Long

068201 Influence of carbon coating on the electrochemical performance of SiO@C/graphite composite anode materials

Hao Lu, Junyang Wang, Bonan Liu, Geng Chu, Ge Zhou, Fei Luo, Jieyun Zheng, Xiqian Yu and Hong Li

068202 Improved electrochemical performance of Li(Ni_{0.6}Co_{0.2}Mn_{0.2})O₂ at high charging cut-off voltage with Li_{1.4}Al_{0.4}Ti_{1.6}(PO₄)₃ surface coating

Yi Wang, Bo-Nan Liu, Ge Zhou, Kai-Hui Nie, Jie-Nan Zhang, Xi-Qian Yu and Hong Li

- 068501 Development of 0.5-V Josephson junction array devices for quantum voltage standards**
Lanruo Wang, Jinjin Li, Wenhui Cao, Yuan Zhong and Zhonghua Zhang
- 068502 Dark count rate and band to band tunneling optimization for single photon avalanche diode topologies**
Taha Haddadifam and Mohammad Azim Karami
- 068503 Research on SEE mitigation techniques using back junction and p^+ buffer layer in domestic non-DTI SiGe HBTs by TCAD**
Jia-Nan Wei, Chao-Hui He, Pei Li and Yong-Hong Li
- 068504 Design and fabrication of 10-kV silicon–carbide p-channel IGBTs with hexagonal cells and step space modulated junction termination extension**
Zheng-Xin Wen, Feng Zhang, Zhan-Wei Shen, Jun Chen, Ya-Wei He, Guo-Guo Yan, Xing-Fang Liu, Wan-Shun Zhao, Lei Wang, Guo-Sheng Sun and Yi-Ping Zeng
- 068701 Theoretical study of overstretching DNA–RNA hybrid duplex**
Dong-Ni Yang, Zhen-Sheng Zhong, Wen-Zhao Liu, Thitima Rujiralai and Jie Ma
- 068901 Uncovering offline event similarity of online friends by constructing null models**
Wenkuo Cui, Jing Xiao, Ting Li and Xiaoke Xu

JUST FOR AUTHORS
— CHINESE PHYSICS B